Applying an isotope-enabled regional climate model over the Greenland ice sheet: effect of spatial resolution on model bias

Marcus Breil[1], E. Christner[1], A. Cauquoin[2,3], M. Werner[2], G. Schädler[1]

[1]Institute of Meteorology and Climate Research, Karlsruhe Institute of Technology, Eggenstein-Leopoldshafen, Germany
[2]Alfred Wegener Institute, Helmholtz Centre for Polar and Marine Sciences, Bremerhaven, Germany
[3]Institute of Industrial Science, University of Tokyo, Kashiwa, Japan

Correspondence to: Marcus Breil (marcus.breil@kit.edu)

Abstract. In order to investigate the impact of spatial resolution on the discrepancy between simulated $\delta^{18}O$ and observed $\delta^{18}O$ in Greenland ice cores, regional climate simulations are performed with the isotope-enabled Regional Climate Model (RCM) COSMO_iso. For this purpose, isotope-enabled General Circulation Model (GCM) simulations with ECHAM5-wiso under present-day and MPI-ESM-wiso under mid-Holocene conditions are dynamically downscaled with COSMO_iso for the Arctic region. The capability of COSMO_iso to reproduce observed isotopic ratios in Greenland ice cores for these two periods is investigated by comparing the simulation results to measured $\delta^{18}O$ ratios from snow pit samples, GNIP stations and ice cores. To our knowledge, this is the first time that a mid-Holocene isotope-enabled RCM simulation is performed for the Arctic region.

Under present-day conditions, a dynamical downscaling of ECHAM5-wiso with COSMO_iso to a spatial resolution of 50 km improves the agreement with the measured $\delta^{18}O$ ratios for 14 of 19 observational data sets. A further increase in the spatial resolution to 7 km yields improvements only for the coastal areas with its complex terrain. For the mid-Holocene, a fully coupled MPI-ESM-wiso time slice simulation is downscaled with COSMO_iso to a spatial resolution of 50 km. In the mid-Holocene, MPI-ESM-wiso already agrees well with observations in Greenland and a downscaling with COSMO_iso does not further improve the model-data agreement. Despite this lack of improvements in model biases, the study shows that in both periods, observed $\delta^{18}O$ values at measurement sites constitute isotope ratios which are mainly within the subgrid-scale variability of the global ECHAM5-wiso and MPI-ESM-wiso simulation results. The correct $\delta^{18}O$ ratios are consequently already included but not resolved in the GCM simulation results and just need to be extracted by a refinement with an RCM. In this context, the RCM simulations provide a spatial $\delta^{18}O$ distribution by which the effects of local uncertainties can be taken into account in the comparison between point measurements and model outputs. Thus, an isotope-enabled GCM-RCM model chain with realistically implemented fractionating processes, constitutes a useful supplement to reconstruct regional paleo-climate conditions during the mid-Holocene in Greenland. Such model chains might also be applied to reveal the full potential of GCMs in other regions and climate periods, in which large deviations relative to observed isotope ratios are simulated.

1 Introduction

Stable isotopes of water ($HD^{16}O$ and $H_2{}^{18}O$) are fractionated during any phase transition. This fractionating process depends on temperature (Dansgaard, 1953; Craig and Gordon, 1965; Jouzel and Merlivat, 1984), so that water isotopic ratios (expressed here in the usual δ notation, δD and $\delta^{18}O$ with respect to the Vienna Standard Mean Ocean Water V-SMOW) reflect the atmospheric conditions under which the fractionating process took place (Dansgaard, 1964; Merlivat and Jouzel, 1979; Gat, 1996). This process is generally utilized to reconstruct paleo-climate conditions such as past temperature changes, using isotopic ratios stored in climate archives (Dansgaard et al., 1969; Masson-Delmotte et al., 2005; Jouzel, 2013).

In Arctic regions like Greenland, ice cores constitute an exceptional climate archive. Over thousands of years, accumulated snow was solidified to ice, preserving at some locations the water isotopic ratios since the last interglacial period. Climate reconstructions based on these ice cores show that the climate conditions changed considerably in Greenland during the Holocene (here defined as the period between present-day and 12 ka; Marcott et al., 2013). Between the early Holocene and the Holocene Thermal Maximum in the mid-Holocene (6 ka), a pronounced warm phase took place. Since then, temperatures steadily decreased until the late Holocene (Marcott et al., 2013; Moossen et al., 2015). In this context, the mid-Holocene is a period of particular interest, as by that time an Arctic warming had taken place due to orbital forcing variations and their related feedbacks on large-scale climate variations, which exhibits similarities to the strong recent Arctic warming. For Greenland, the mid-Holocene provides the opportunity to investigate the processes leading to this warming, in more detail and to potentially obtain new insights about the future development of the Arctic region (Yoshimori and Suzuki, 2019).

While General Circulation Models (GCMs) are generally able to reproduce the direction and large-scale patterns of past climate changes (e.g. Timm and Timmermann, 2007; Smith and Gregory, 2012), they often fail to reproduce the magnitude of regional changes (Braconnot et al., 2012; Harrison et al., 2014), documented in various local climate archives. Thus, a scale gap might exist between the measured point information and the large-scale climate information generated by GCMs. The comparison of observational and GCM data can therefore be subject to considerable uncertainties (Felzer and Thompson, 2001).

Especially for structured landscapes, the spatial resolution in GCMs is often too coarse to resolve relevant local factors (Jost et al., 2005; Fischer and Jungclaus, 2011). Important properties like topography and surface conditions are consequently only represented in a generalized and imprecise form in climate simulations. In most cases, this does not adequately represent the complex characteristics of the land surface and its associated interactions with the atmosphere. For stable water isotopes, key physical processes of isotope fractionation are therefore not well resolved in coarse resolution GCMs, leading to differences between simulated and observational isotope data, especially in complex terrains (Sturm et al., 2005; Werner et al., 2011). Isotope-enabled GCMs are consequently not able to reproduce regional changes in isotope ratios quantitively (e.g. Risi et al., 2010), and the simulated isotope ratios with GCMs exhibit in many cases larger deviations relative to observed ratios than the results of corresponding Regional Climate Model (RCM) simulations. For instance, Sturm et al., (2007) were able to reduce the bias of simulated isotope ratios in precipitation, by a regional downscaling of an isotope-enabled GCM run in

South America. Comparable results were achieved by Sjolte et al., (2011) for isotope-enabled RCM simulations in Greenland.

Therefore, in the presented study, isotope-enabled GCM simulation results for the Arctic region are dynamically downscaled with an isotope-enabled RCM to a higher temporal and spatial resolution. By means of such regional simulations, the spatial and temporal variability of the isotopic ratios in the Arctic is potentially increased, accounting for the heterogeneity of local conditions at the different ice core locations and the associated uncertainties. In this way, the impact of highly resolved local conditions on the spatial and temporal variability of isotopic ratios is investigated, and the impact of such small-scale variability on the discrepancy between simulated and observed paleo-climate conditions in the Arctic region is examined.

To explore this, the isotope-enabled version of the RCM COSMO-CLM (Rockel et al., 2008), COSMO_iso (Pfahl et al., 2012; Christner et al., 2018), is used. In a first step, the general suitability of COSMO_iso to be used for isotope applications in Greenland is assessed. For this purpose, near-surface temperatures and precipitation amounts simulated with the standard COSMO version are compared with observations in the Arctic region. Subsequently, the capability of COSMO_iso to simulate realistic water isotopic ratios for Greenland is tested by downscaling a global present-day simulation with an isotope-enabled GCM for the Arctic region. The GCM and RCM results are then compared to measured water isotope ratios in precipitation and snow pit samples. Afterwards, the tested isotope-enabled COSMO_iso model system is used to downscale an isotope-enabled GCM simulation for a mid-Holocene time-slice. The simulated isotopic ratios are evaluated against Greenland ice core data. Such a dynamical downscaling of global isotope simulations for Greenland under mid-Holocene conditions, is performed for the first time in the framework of this study.

2 Methods

2.1 COSMO_iso

2.1.1 Model Description

In this study, simulated stable water isotope concentrations of $HD^{16}O$ and $H_2{}^{18}O$ with isotope-enabled GCMs (section 2.1.2), are regionally downscaled with COSMO_iso (Pfahl et al., 2012), an isotope-enabled version of the numerical weather prediction model COSMO (Consortium for Small-scale Modeling; Baldauf et al., 2011) (version 4.18). For the purpose of long-term climate simulations, isotope-routines of COSMO_iso were implemented in COSMO-CLM (Rockel et al., 2008), the climate version of COSMO. In this context, the δD and $\delta^{18}O$ ratios in the soil water and the surface layer snow are simulated with TERRA_iso V.1 (Dütsch, 2017; Christner et al., 2018), the isotope-enabled version of the multi-layer Land Surface Model TERRA-ML (Schrodin and Heise, 2001) in COSMO. In several studies, COSMO_iso and TERRA_iso were successfully employed for the simulation of isotopic ratios in the mid-latitudes (Pfahl et al., 2012; Aemisegger et al., 2015; Christner et al., 2018). In the present study, the model system will be applied to the Arctic region. For this, some additional modifications regarding the treatment of snow and ice had to be implemented in the model:

Snow albedo

The surface albedo of fresh snow is increased from 0.7 to 0.8 to improve the model agreement with measured values of short-wave reflectance and 2m temperature at stations from the Cooperative Institute for Research in Environmental Sciences at the University of Colorado Boulder (CIRES) in Central Greenland.

Snow layer thickness

In the standard configuration of COSMO, the Greenland ice sheet is treated as a constant mass of ice, which is covered by a single snow layer. But in this model structure, dynamical processes within the ice sheet (flow, basal melt) are not included. As a result, the depth of the snow layer is constantly increasing and thus also its heat capacity. To avoid this spurious model behaviour, the snow layer depth is limited to 5 cm in this study. Using this value, realistic diurnal cycles of the 2 m air temperature could be simulated.

Marine regions with sea ice cover

To be able to simulate reasonable fractionation processes for marine regions with sea ice cover, a snow layer is also implemented on top of the sea ice (e.g., as suggested in Bonne et al., 2019). The isotopic composition of this surface snow layer is in this case set to the isotopic composition of the most recent precipitation.

Fractionation at snow covered surfaces

Isotope fractionation during sublimation from a surface snow layer is poorly understood. Several different processes are suggested to be involved, which are not yet taken into account in state-of-the-art isotope enabled models (see e.g. discussion in Christner et al., 2017), such as non-fractionating layer-by-layer sublimation (e.g. Ambach et al., 1968), kinetic fractionation during sublimation into sub-saturated air, a diurnal cycle of sublimation combined with fractionating vapor deposition on the snow (e.g. Steen-Larsen et al., 2014), and fractionating melt water evaporation combined with recrystallization of residual melt water have been suggested (Gurney and Lawrence, 2004). To approximate this complex interplay of different influencing factors, in this study, an equilibrium fractionation during sublimation from surface layer snow and sea ice is assumed. However, the authors are aware that this is just a simplified description of isotope fractionation during sublimation.

2.1.2 Model Simulation Setup

The capability of COSMO_iso to realistically reproduce the fractionating processes of stable water isotopes in Greenland is evaluated. For this, the nudged simulation outputs (standard and isotopic) from an isotope-enabled atmospheric model ECHAM5-wiso (Werner et al., 2011) simulation are dynamically downscaled with COSMO_iso for the whole Arctic region. The data from the same ECHAM5-wiso simulation have been already used as boundary conditions for COSMO_iso simulations over Europe by Christner et al. (2018). The simulation outputs from ECHAM5-wiso are at a T106 horizontal spatial resolution (1.1° x 1.1°) and on 31 atmospheric vertical levels. The dynamical fields were nudged every 6 hours towards ERA-Interim reanalysis data (Dee et al., 2011). Monthly varying sea surface temperatures and sea ice cover were prescribed as lower boundaries over sea, also based on the ERA-Interim data. The simulation period is 2008-2014. The spatial resolution of COSMO_iso is 0.44° x 0.44°, corresponding to 50 km x 50 km in rotated coordinates (COSMO_iso_50km). Afterwards, an additional COSMO_iso simulation with a spatial resolution of 0.0625° x 0.0625° (corresponding to about 7 km × 7 km) for Greenland (COSMO_iso_7km) is nested in the COSMO_iso_50km simulation. This high-resolution simulation covers the year 2011. In the COSMO_iso runs, the horizontal wind fields above the 850 hPa level are spectrally nudged (von Storch et al., 2000) towards the reanalysis-based dynamical fields of ECHAM5-wiso. This method ensures that consistent atmospheric boundary conditions build the framework for the fractionating processes simulated in COSMO_iso. The model domains of both simulations is shown in Figure 1.

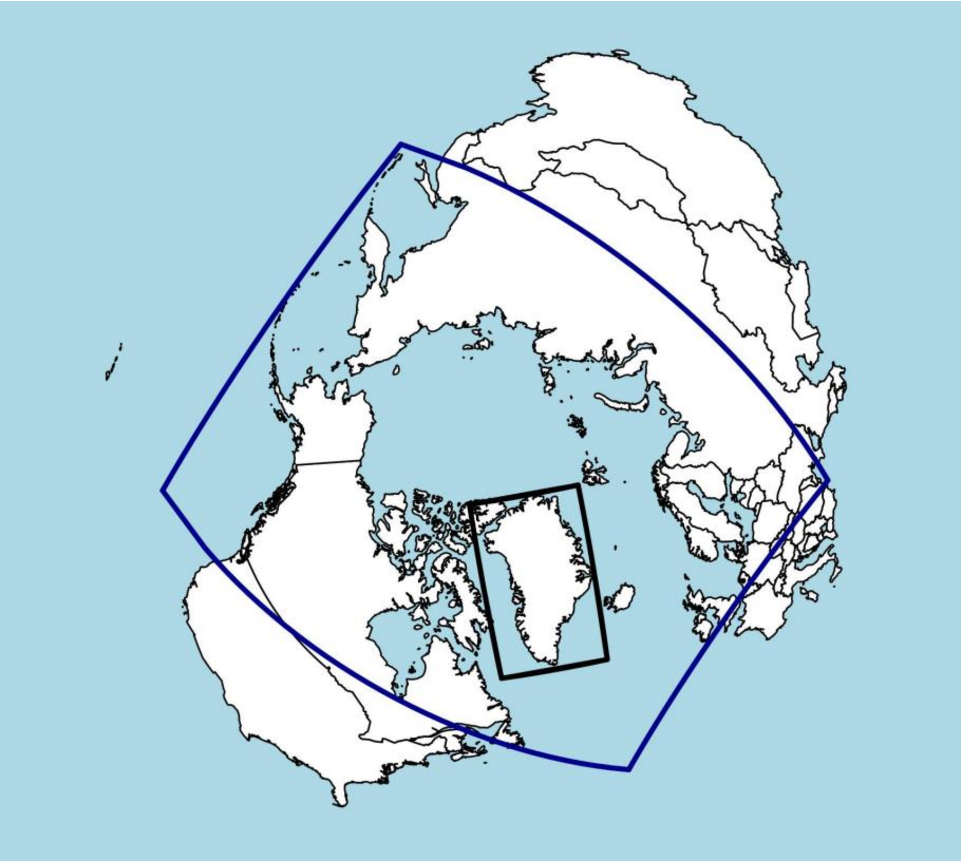

Figure 1: COSMO_iso model domain of the 50 km (blue) and the 7 km (black) simulation.

The same model chain is applied to the mid-Holocene period. Atmospheric fields have been retrieved from a mid-Holocene simulation of the fully-coupled isotope-enabled Max Planck Institute Earth System Model (MPI-ESM-wiso, Cauquoin et al., 2019), whose atmospheric component is ECHAM6-wiso. The major ECHAM6 model changes compared to ECHAM5 include an improved representation of radiative transfer in the solar part of the spectrum, an improved representation of surface albedo, a new aerosol climatology and an improved representation of the middle atmosphere (Stevens et al., 2013). The ocean component is the Max Planck Institute Ocean-Model (MPIOM, Jungclaus et al., 2013). With COSMO_iso, a representative time slice of 30 years is simulated for this climate period, only, since the regional COSMO_iso simulations are computationally very expensive. The greenhouse gas concentrations and the orbital parameters are adapted, according to the Paleoclimate Modelling Intercomparison Project 4 experiment design (PMIP4, Kageyama et al., 2018). The model domain of the COSMO_iso simulations is identical to the present-day simulations.

2.2 Observations

The capability of the isotope-enabled regional climate model COSMO_iso to reproduce measured isotopic ratios in Greenland is evaluated by comparing the simulation results to observational data. The simulated isotopic composition in precipitation is assessed by comparing the model results in the arctic region with observed monthly data from the Global Network of Isotopes in Precipitation (GNIP) of the International Atomic Energy Agency and the World Meteorology Organization [IAEA/WMO, 2016] over the period 2008-2014 (Table 1). Furthermore, simulated $\delta^{18}O$ ratios are compared to snow pit samples collected during the North Greenland Traverse (Fischer et al., 1998; Weißbach et al., 2016a) and top core samples from five ice core locations (Renland (Vinther et al., 2008), Neem (Masson-Delmotte et al., 2015), GISP2 (Grootes and Stuiver, 1997), Summit (Fischer, 2003), SE-Dome (Furukawa et al., 2017)). The station numbers assigned to the respective samples within this study, as well as their locations and $\delta^{18}O$ values are summarized in Table 2. Since all snow pit samples cover different time periods, the present-day $\delta^{18}O$ values (black numbers in Table 2) are calculated as an average of all available $\delta^{18}O$ values measured between 1940 and 2014. With this procedure uncertainties in snow pit samples and top ice core samples, associated with post depositional diffusion and wind erosion and the resulting constraints in analysing annual and interannual top ice core data (e.g. Johnson et al., 2000), can be neglected. However, further uncertainties in snow pit samples and ice core data remain, regarding the timescale assignment (Steig et al., 2005) and the spatial variability (Weißbach et al., 2016b).

Since both, snow pit samples and top core samples from ice cores represent an integrated signal of the isotopic composition in precipitation, the observed isotope ratios are compared with simulated yearly mean $\delta^{18}O$ values in precipitation. For the calculation of this yearly mean values, the modelled $\delta^{18}O$ in precipitation is weighted with accumulation rate, i.e. months with high precipitation amounts get a higher weight compared to months with small precipitation amounts.

Table 1: List of GNIP stations used in this study.

No.	Station Name	Longitude	Latitude	Time period
1	Danmarkshavn	-18.66	76.76	2008-2014
2	Ny Alesund	-11.93	78.91	2008-2014
3	Reykjavik	-21.93	64.13	2008-2014
4	Espoo	24.83	60.18	2008-2010
5	Kuopio	27.62	62.89	2008-2010
6	Rovaniemi	25.75	66.49	2008-2010
7	Snare Rapids	-116.00	63.52	2008-2010
8	Tartu	26.46	58.26	2013-2014
9	Vilsandi	21.81	58.38	2013-2014

Table 2: Description of the snow pit and ice core samples used in this study. The present-day $\delta^{18}O$ values are calculated as an average of all available $\delta^{18}O$ values measured in snow pit samples between 1940-2014. The mid-Holocene $\delta^{18}O$ values are calculated as an average of the measured $\delta^{18}O$ values in ice cores over the period 5.5 ka – 6.5 ka. Black numbers indicate present-day $\delta^{18}O$ values, blue numbers mid-Holocene values.

No.	Name	Sample	Longitude	Latitude	$\delta^{18}O$	Reference
1	Renland	top core	-26.73	71.27	-27.38 (-26.44)	Vinther et al., 2008
2	NEEM	top core	-51.06	77.45	-33.24	Masson-Delmotte et al., 2015
3	GISP2	top core	-38.48	72.58	-34.95 (-34.83)	Grootes & Stuiver, 1997
4	Summit	top core	-37.64	73.03	-36.46	Fischer, 2003
5	B27_B28	snow pit	-46.48	76.65	-34.05	Weißbach et al., 2016a
6	NGT03C93	snow pit	-37.62	73.94	-37.02	Weißbach et al., 2016a
7	NGT06C93	snow pit	-37.62	75.25	-36.89	Weißbach et al., 2016a
8	NGT14C93	snow pit	-36.4	76.61	-36.18	Weißbach et al., 2016a
9	NGT23C94	snow pit	-36.5	78.83	-35.18	Weißbach et al., 2016a
10	NGT27C94	snow pit	-41.13	80	-34.01	Weißbach et al., 2016a
11	NGT30C94	snow pit	-45.91	79.34	-34.19	Weißbach et al., 2016a
12	NGT33C94	snow pit	-44	78	-36.13	Weißbach et al., 2016a
13	NGT37C95	snow pit	-49.21	77.25	-33,81	Weißbach et al., 2016a
14	NGT39C95	snow pit	-46.48	76.65	-34.95	Weißbach et al., 2016a
15	NGT42C95	snow pit	-43.49	76	-35.53	Weißbach et al., 2016a
16	NGT45C95	snow pit	-42	75	-35.33	Weißbach et al., 2016a
17	GRIP	top core	-37.64	72.58	-35.23 (-34.73)	Vinther et al., 2006
18	NGRIP	top core	-42.32	75.1	-35.15 (-34.69)	Vinther et al., 2006
19	SE-Dome	top core	-36.37	67.18	- 27.26	Furukawa et al., 2017

Ice core samples are also used to evaluate the simulated isotopic ratios for the mid-Holocene. Beside the already mentioned Renland and GISP2 samples, two more ice core samples, namely GRIP and NGRIP (Vinther et al., 2006), are used for the model evaluation. The mid-Holocene $\delta^{18}O$ values (blue numbers in Table 2) are calculated as an average of the measured $\delta^{18}O$ values in ice cores over the period 5.5 ka – 6.5 ka.

3 Results

3.1 Present-Day

3.1.1 Standard climatological parameter

In a first step, the general capability of the COSMO model to reproduce observed standard climatological parameters in present-day simulations for Greenland is assessed. For this purpose, the results of an ERA-Interim reanalysis (Dee et al., 2011) driven simulation with the standard COSMO model (without isotope application) are compared with observations, collected by the Danish Meteorological Institute (DMI). Evaluated are the yearly mean 2 m temperatures (Figure 2a) and the yearly mean precipitation sums (Figure 2b) over the period 1995 – 2015. Both, simulated 2 m temperatures as well as simulated precipitation amounts are in good agreement with the DMI observations. Especially the simulated 2 m temperatures coincide well with the observed values. For the precipitation sums, the spread of simulated and observed values is higher than for the 2 m temperatures, a feature generally occurring in weather and climate simulations. Thus, the COSMO model is generally able to simulate reasonable climate conditions in Greenland and can therefore be used for isotope applications in this region. A detailed analysis of the standard COSMO model performance in the Arctic region is presented in Karremann et al., (2020).

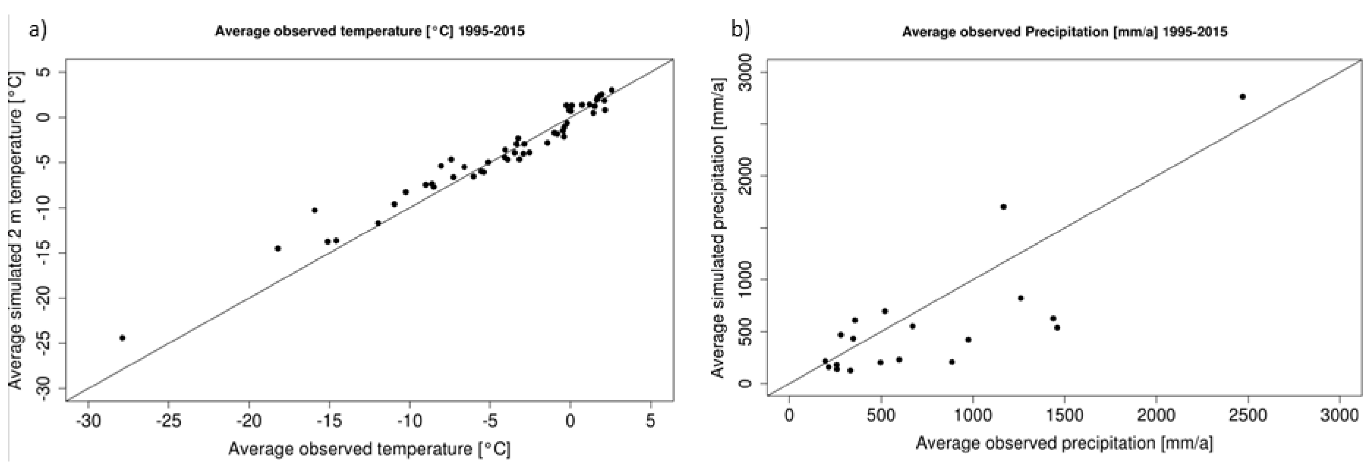

Figure 2: Simulated yearly mean (a) 2 m temperatures and (b) precipitation sums of a standard COSMO simulation, driven with ERA-Interim, for Greenland over the period 1995-2015 compared to DMI observations.

3.1.2 Comparison of simulated $\delta^{18}O$ data to station data

Figure 3 shows the yearly mean $\delta^{18}O$ values for the period 2008-2014 for Greenland, simulated with COSMO_iso_50km (a) and ECHAM5-wiso (b). Additionally, the locations and the observed $\delta^{18}O$ values of the 19 snow pit samples, used to assess the models' capability to reproduce observed $\delta^{18}O$ ratios in Greenland, are illustrated. In general, COSMO_iso in a 50 km x 50 km spatial resolution is able to reflect the observed isotopic ratios at the snow pit samples and improves the simulation results of ECHAM5-wiso. In both simulations, the $\delta^{18}O$ ratios are high near the coastline and low in Central Greenland. But in COSMO_iso_50km, the $\delta^{18}O$ ratios decline more rapidly from the coastline to the inland plateau than in ECHAM5-wiso. The spatial $\delta^{18}O$ differences are consequently more pronounced and the general overestimation of $\delta^{18}O$ ratios, which occurs in ECHAM5-wiso, is reduced in COSMO_iso_50km. As a consequence, the regional simulation reaches a better agreement with the observations. The average bias reduction of COSMO_iso_50km over all snow pit samples is 0.7 ‰. Especially for the snow pit samples for which ECHAM5-wiso exhibits strong deviations from the observed $\delta^{18}O$ values (1,3,4,6,7,8,9,10,16,17,19; see Table 2), a regional downscaling with COSMO_iso_50km reduces the bias considerably (Figure 4). But for snow pit samples at which ECHAM5-wiso has already a high agreement with the observations (2,5,11,13,14), COSMO_iso_50km tends to increase the bias.

Figure 5 shows that these annual biases of the COSMO_iso_50km simulation are not caused by systematic seasonal biases, as for example reported by Sjolte et al., (2011) for RCM simulations in Greenland. Shown are the simulated monthly $\delta^{18}O$ values with COSMO_iso_50km compared to observed monthly $\delta^{18}O$ values in precipitation for the period 2008-2014, collected at arctic stations of the GNIP dataset (Table 1). In general, the modelled $\delta^{18}O$ values in precipitation are in good agreement with the monthly GNIP data. But in the COSMO_iso_50km simulation no systematic over- or underestimation of observed isotope ratios is simulated with the RCM. This is true for each season. Neither in winter (low $\delta^{18}O$ values), nor in summer (high $\delta^{18}O$ values), systematic deviations to the observations are simulated. Thus, the seasonal variability in the COSMO_iso_50km results has no systematic impact on the yearly mean $\delta^{18}O$ values and is therefore not the reason for systematic differences between the coarse model results and observations.

As visible in Figure 3, these systematic differences are rather caused by a southward shift of the area of low yearly mean $\delta^{18}O$ values in central Northern Greenland in COSMO_iso_50km relative to ECHAM5-wiso. As a result, the simulated $\delta^{18}O$ values in central Northern Greenland in COSMO_iso_50km are higher than in ECHAM5-wiso. Since there, ECHAM5-wiso has already a high agreement with the observed $\delta^{18}O$ values, a model bias is introduced in COSMO_iso_50km, causing the deviations relative to the observations in Northern Greenland.

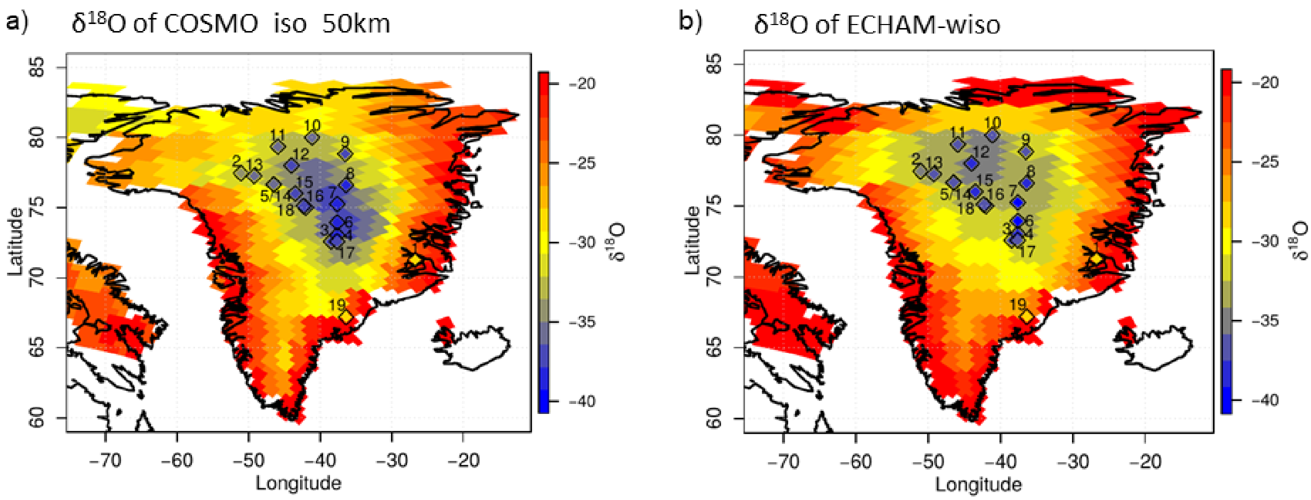

Figure 3: Yearly mean $\delta^{18}O$ values of COSMO_iso_50km (a) and ECHAM5-wiso (b, interpolated to the COSMO_iso_50km grid) for the period 2008 - 2014 and the corresponding observations for the 19 snow pit samples (Table 2).

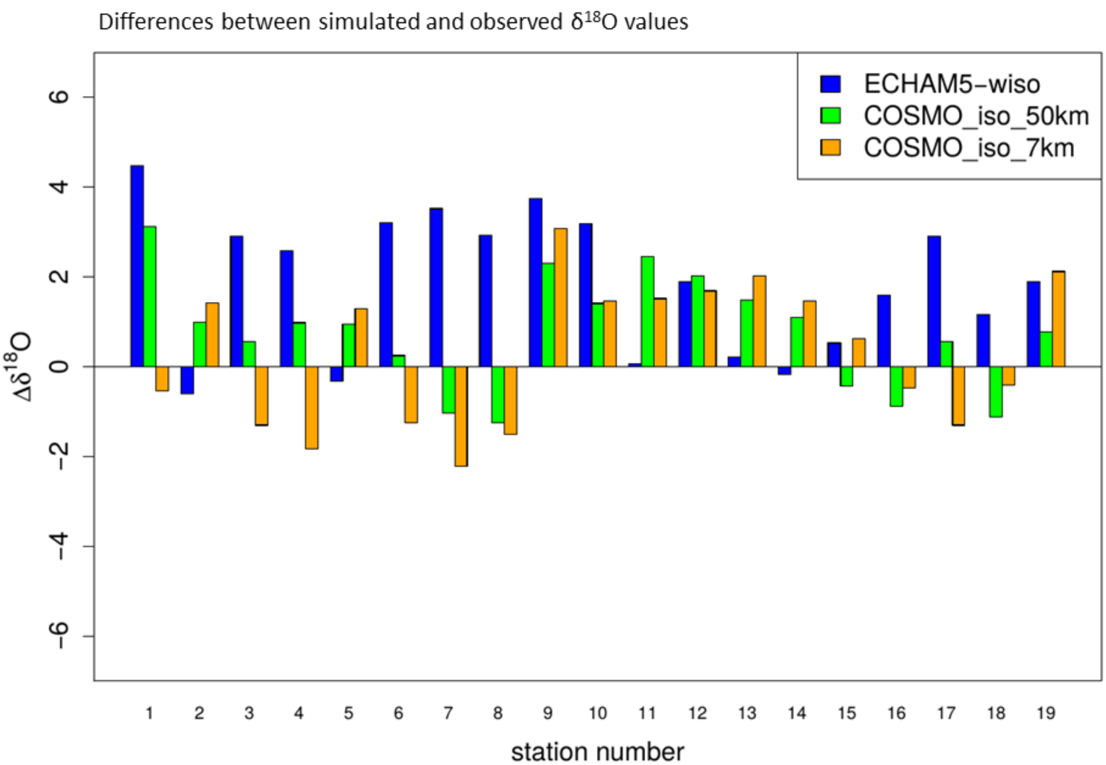

Figure 4: Differences (Δ) between simulated and observed $\delta^{18}O$ values (model minus observation) for the model results of ECHAM5-wiso, COSMO_iso_50km, and COSMO_iso_7km, and snow pit samples / top core samples from ice cores from Greenland (simulation: 2011, observation: mean present values). Numbers refer to the different snow pit locations shown in Figure 3.

A further downscaling with COSMO_iso to a spatial resolution of 7 km x 7 km does not improve the simulation results further. The average bias reduction in comparison to ECHAM5-wiso is 0.6 ‰. The only exception constitutes the snow pit sample from Renland (1). Here, a considerable model bias in ECHAM5-wiso and COSMO_iso_50km is strongly reduced in COSMO_iso_7km. The coastal area of Renland is characterized by complex terrain and constitutes a special case for isotope-enabled modeling in Greenland. The snow pit sample is located in a transition zone from the homogeneous inland glaciation to the rugged coastline, where the glaciers calve into the sea. Thus, within short distances large differences in altitude and land surface characteristics occur in this region. The isotopic ratios in the snow pit sample are therefore strongly affected by these heterogeneous local conditions, which are insufficiently represented in the coarse model resolution of ECHAM5-wiso. By increasing the spatial resolution with regional climate modelling, also the representation of the associated small-scale processes is improved. This leads generally to an improved agreement of the simulation results with observations, as seen for the COSMO_iso_7km run for Renland (Figure 4).

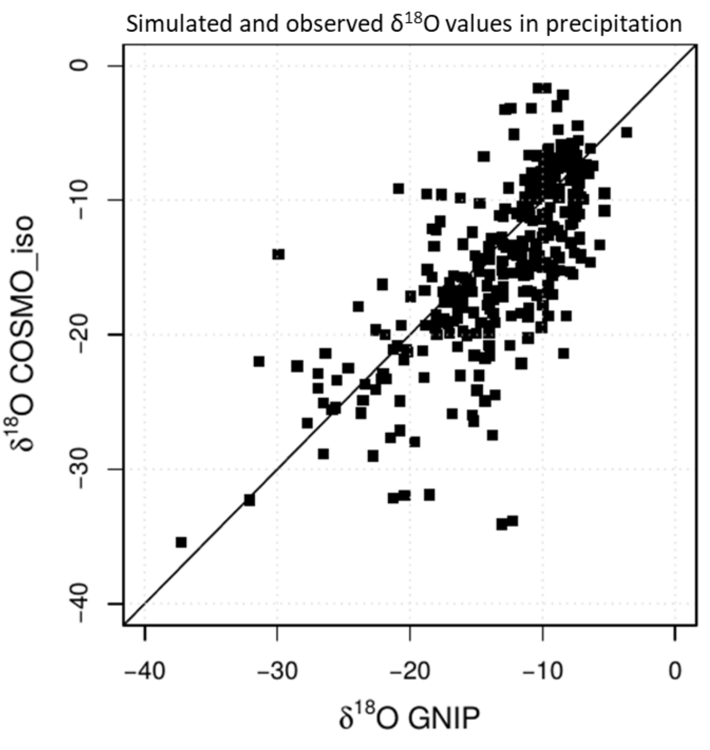

Figure 5: Monthly $\delta^{18}O$ simulated with COSMO_iso_50km for the period 2008 - 2014 and the corresponding observations for 9 GNIP stations (Table 1).

However, an increase in spatial resolution is also associated with an increased heterogeneity of the surface characteristics and the related small-scale processes, especially in complex terrains. This is because the GCM grid boxes are further divided in smaller RCM grid boxes and consequently higher as well as lower values (for e.g. altitude) are now included in the respective GCM grid boxes. As a consequence, an additional spatial variability is introduced in the RCM simulations in comparison to the GCM results. Due to uncertainties accompanied by model simulations, this can potentially increase the RCM bias with respect to in situ point measurements, which may actually be closer to the spatially averaged values simulated by the coarse GCM model. This effect can be observed for the SE-Dome ice core (19) in southeastern Greenland. Comparable to the Renland ice core, SE-Dome is located near the coastline. But in contrast to the Renland ice core, an increase in the spatial resolution to 7 km does not further improve the RCM results for SE-Dome. On the contrary, the $\delta^{18}O$ bias is even higher than in the ECHAM5-wiso simulation.

However, by performing higher resolved RCM simulations, the subgrid-scale variability of $\delta^{18}O$ within GCM grid boxes can be simulated and compared to observed $\delta^{18}O$ values. In this way, the inherent uncertainty of in situ measurements, associated with a local micrometeorological variability, can be considered. Thus, in the following, snow pit samples are not anymore solely compared to the model grid boxes covering the samples location. Instead, it is investigated whether the $\delta^{18}O$ range of all adjacent RCM grid boxes to a snow pit location is consistent with the observed $\delta^{18}O$ value of the same site. For this, all RCM grid boxes located within the corresponding GCM grid box are included in the comparison with the observations.

3.1.3 $\delta^{18}O$ variability

The spatial isotopic ratio variability of the COSMO_iso_50km grid boxes surrounding the 19 snow pit samples is shown as a Box-Whiskers-plot in Figure 6a. The spatial isotopic ratio variability of the COSMO_iso_7km is shown in Figure 6b. In this spatial isotopic ratio variability, the $\delta^{18}O$ values of all COSMO_iso (50 km) and COSMO_iso (7 km) grid boxes within the ECHAM5_wiso grid box closest to the snow pit sample, are included. For 14 of the 19 snow pit samples (1,2,3,4,5,6,7,8,14,15,16,17,18,19) the observed $\delta^{18}O$ values are within the range of the spatial COSMO_iso_50km grid box variability. But for 5 of the 19 snow pit samples (9-13) the spatial isotope range of the COSMO_iso_50km simulation does not fit with the observations. Since these stations are all located in the north of Greenland (Figure 3), this is most likely associated with the southward shift of the area of low yearly mean $\delta^{18}O$ values in central Northern Greenland in COSMO_iso_50km in comparison to ECHAM5-wiso, as already described in section 3.1.2.

A downscaling to 7 km does slightly increase the spread of the COSMO_iso results. But still, the observed $\delta^{18}O$ values from 5 of 19 snow pit samples are not covered within the modelled COSMO_iso_7km grid box variability (Figure 6b). Thus, a further downscaling to a spatial resolution of 7 km does not increase the accuracy of the simulated isotopic ratio spread within an ECHAM5-wiso grid box. In accordance with the missing benefits of the COSMO_iso_7km simulation and its increased computing time costs, only a COSMO_iso_50km simulation is performed for the mid-Holocene (section 3.2).

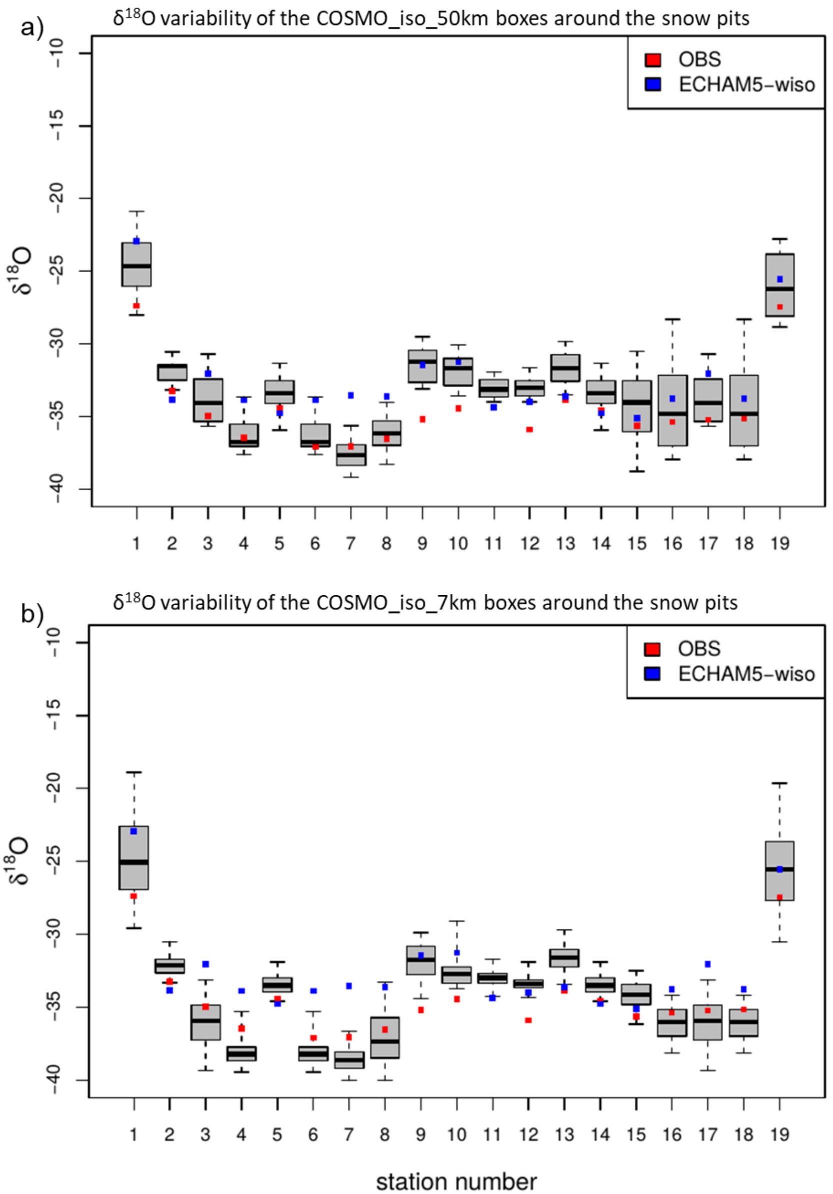

Figure 6: Present-day isotopic ratio variability of the COSMO_iso grid boxes, surrounding the 16 snow pit samples for the (a) 50 km and (b) 7 km simulation. The black bar in the Box-Whiskers-plot represents the median of the isotope ratio distribution. The box comprises the upper and lower quartile, the whiskers the whole distribution. The MPI-ESM-wiso results are shown by the blue dots and the observed $\delta^{18}O$ values are shown by the red dots.

The high spatial $\delta^{18}O$ variability in COSMO_iso simulations is also reflected in the spatial $\delta^{18}O$-temperature slope of the COSMO_iso_50km run (Figure 7c), a measure that is frequently used to analyze how strong isotope ratios and surface temperatures are interrelated. The spatial isotope-temperature slope constitutes a linear fit between the simulated $\delta^{18}O$ ratios and the surface temperatures at all COSMO_iso_50km grid boxes within the respective ECHAM5-wiso grid box. The spatial δ^{18}O-temperature slope is high in Central Greenland and low at the coastline. In order to better understand these spatial δ^{18}O-temperature patterns, both quantities affecting the spatial δ^{18}O-temperature slope, i.e. the spatial δ^{18}O variability and the spatial temperature variability, are explicitly analyzed in Figure 7a and Figure 7b. These spatial variabilities are calculated as the standard deviation of all COSMO_iso_50km grid boxes within the respective ECHAM5-wiso grid boxes.

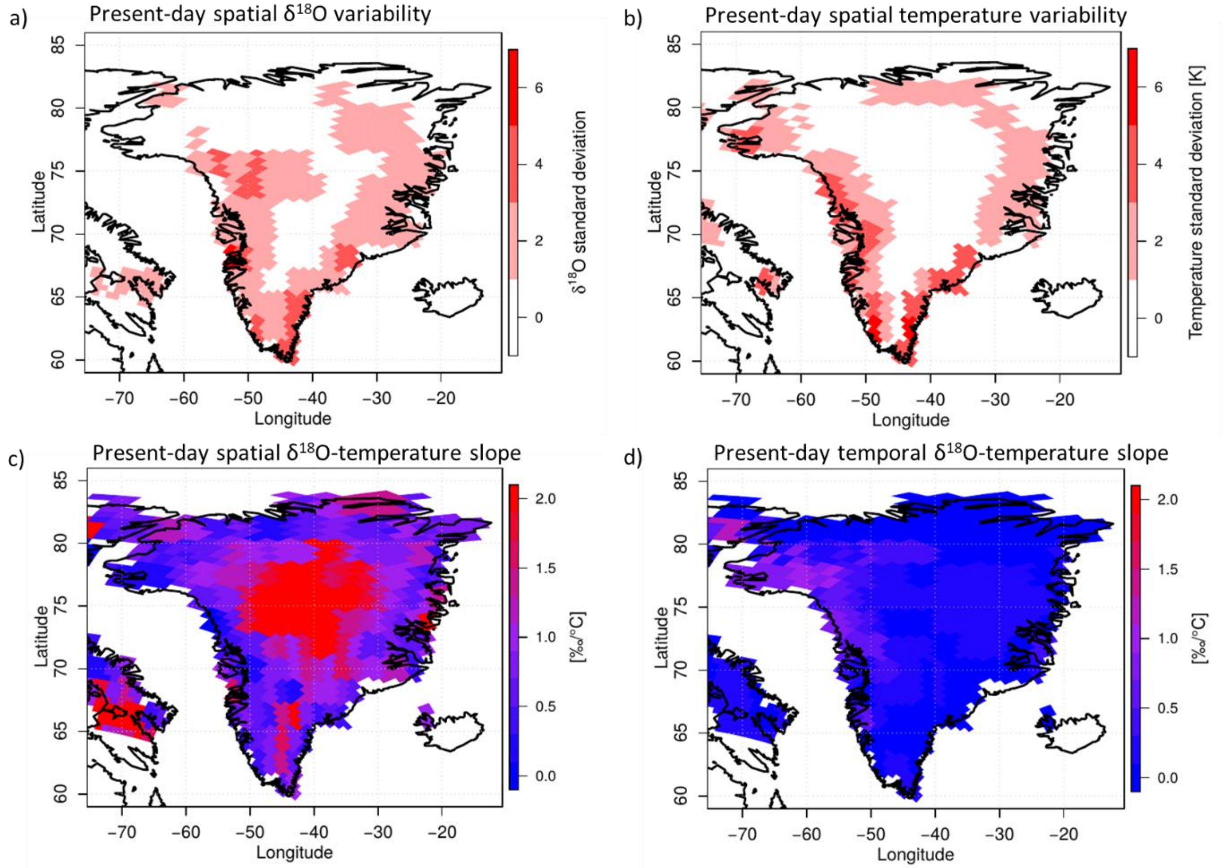

Figure 7: Present-day spatial subgrid-scale variability (calculated as standard deviation) of (a) δ^{18}O and (b) surface temperature, derived from the COSMO_iso_50km grid boxes within the respective ECHAM5-wiso grid boxes for whole Greenland. Present-day (c) spatial and (d) interannual temporal δ^{18}O-temperature slope for Greenland, based on yearly mean values.

Figure 7a shows that at the coastline, the spatial δ^{18}O variability of COSMO_iso_50km is considerably increased within the ECHAM5-wiso grid boxes. In Central Greenland the increase in the spatial isotopic ratio variability is lower. Thus, the simulated spatial δ^{18}O variability is high in regions where large orographic differences occur within short distances, like the coastal areas of Greenland, and lower for homogeneous terrain like the inland plateau. Nevertheless, widespread areas with higher spatial isotopic variability occur also in the inland plateau of Greenland. This is not the case for the spatial surface temperature variability. In Central Greenland almost no surface temperature variability occurs (Figure 7b). But near the coastline the spatial surface temperature variability is also high, highlighting how important the land surface characteristics are for the regional temperature variability. The low spatial $\delta^{18}O$-temperature slope at the coastline (Figure 7c) is therefore a result of a high surface temperature variability in this region counteracting the high $\delta^{18}O$ variability in the slope calculation. On the contrary, the $\delta^{18}O$-temperature slope is high in Central Greenland due to an increased $\delta^{18}O$ variability there, while the surface temperature variability is low. The spatial distribution of $\delta^{18}O$ consequently not only depends on land surface processes, but also on dynamic atmospheric processes. In this way, isotopic ratios based on atmospheric fractionation processes along the trajectory of an air mass, are transported to Central Greenland and increase there the isotopic variability.

In order to investigate the temporal interrelations between the isotope ratios and the surface temperature, the interannual temporal $\delta^{18}O$-temperature slope is calculated for the COSMO_iso_50km simulation, based on the yearly mean $\delta^{18}O$ and surface temperature values (Figure 7d). The interannual temporal $\delta^{18}O$-temperature slope is, in contrast to the spatial $\delta^{18}O$-temperature slope, very small all over Greenland, which is in accordance with the results of Sjolte et al., (2011). That means that the interannual $\delta^{18}O$ variability is less pronounced than the interannual surface temperature variability and both quantities are lowly correlated. The impact of interannual surface temperature variations on the temporal $\delta^{18}O$ variability is therefore small in Greenland.

3.2 Mid-Holocene

3.2.1 Comparison of simulated $\delta^{18}O$ data to ice core data

In contrast to the present-day simulations, for the mid-Holocene, COSMO_iso_50km is not anymore driven by ECHAM5-wiso, but by MPI-ESM-wiso. While in ECHAM5-wiso oceanic boundary conditions are prescribed by monthly varying sea surface temperatures and sea ice cover, ocean states are calculated internally in the fully-coupled atmosphere-ocean Earth-System-Model MPI-ESM-wiso. Systematic deviations between the COSMO_iso_50km simulations for mid-Holocene and present-day, caused by these different forcing approaches, therefore, cannot be excluded. For this reason, a comparison of the mid-Holocene $\delta^{18}O$ anomalies to the present-day conditions is omitted and an analysis is performed for simulated absolute $\delta^{18}O$ ratios and their differences to observed $\delta^{18}O$ values.

In Figure 8a the absolute differences of the simulated MPI-ESM-wiso (blue) and COSMO_iso_50km (green) grid box results to the observed $\delta^{18}O$ ratios at the corresponding ice cores are presented for the mid-Holocene. As in Figure 6, the spatial isotopic ratio variability of the COSMO_iso_50km grid boxes surrounding four Greenland ice core samples is shown as a Box-Whiskers-plot. MPI-ESM-wiso properly reflects the isotopic ratios of the mid-Holocene from ice core data. For the inland ice cores (GRIP, GISP2, NGRIP), the simulated $\delta^{18}O$ deviates only about 1 ‰ to the observations, at Renland the deviation is about 3 ‰. For GRIP and GISP2 the MPI-ESM-wiso simulations slightly underestimate the $\delta^{18}O$ ratios, for NGRIP and Renland, the $\delta^{18}O$ values are slightly overestimated.

COSMO_iso_50km simulates the opposite sign of MPI-ESM-wiso for the deviation of the $\delta^{18}O$ values to the observations at the inland ice cores. That means that in GRIP and GISP2, the underestimated $\delta^{18}O$ values in MPI-ESM-wiso are turned into overestimated $\delta^{18}O$ values in COSMO_iso_50km, at NGRIP the overestimation is turned into an underestimation, but the net bias is not reduced. At Renland, the bias is even increased. Thus, by just looking at the absolute biases, the downscaling does not seem to bring an added value to the MPI-ESM-wiso results for mid-Holocene conditions. But taking also into account the spatial isotopic ratio variability in the COSMO_iso_50km simulation, the model results are in agreement with the isotopic ratios of the ice core samples.

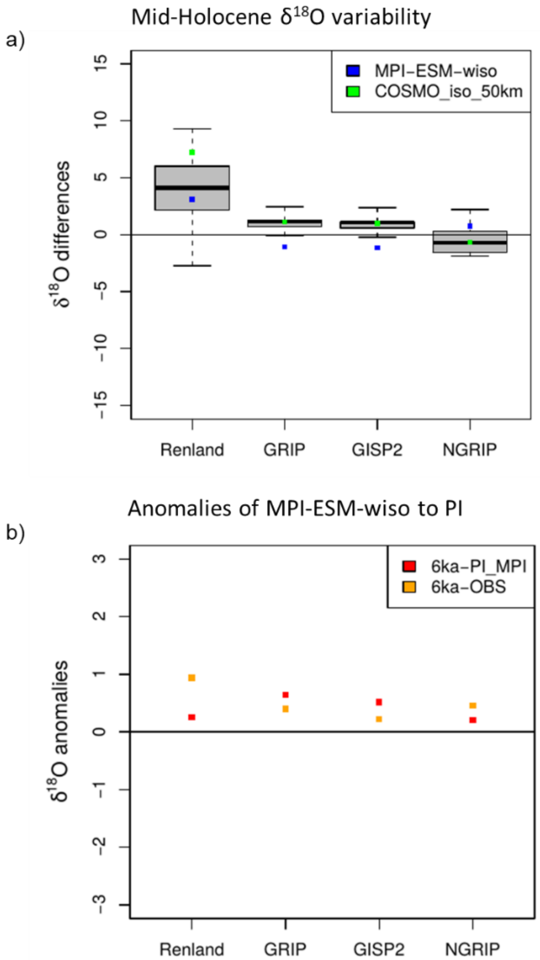

Figure 8: (a) mid-Holocene isotopic ratio variability of the COSMO_iso_50km grid boxes surrounding four Greenland ice core samples. In each grid box, the simulated δ^{18}O ratios are subtracted by the observed ratios in the ice cores. The black bar in the Box-Whiskers-plot represents the median of the isotope ratio distribution. The box comprises the upper and lower quartile, the whiskers the whole distribution. The MPI-ESM-wiso (blue dots) and COSMO_iso_50km (green dots) results for the grid points closest to the ice cores are also shown as differences to the observed δ^{18}O ratios. (b) the anomalies of the MPI-ESM-wiso simulation to the pre-industrial (PI) conditions, based on an MPI-ESM-wiso PI-reference simulation (Cauquoin et al., 2019) are shown in red dots, the observed mid-Holocene-PI anomalies in orange dots.

In Figure 8b, the MPI-ESM-wiso model anomalies with reference to the pre-industrial period (PI) conditions, which are based on an MPI-ESM-wiso PI-reference simulation performed by Cauquoin et al. (2019), are compared to the measured mid-Holocene-PI $\delta^{18}O$ anomalies of the ice cores. The positive $\delta^{18}O$ anomalies between mid-Holocene and PI for both ice core data and MPI-ESM-wiso model results are associated with higher temperatures, especially during the summer and a reduction in Arctic sea-ice during mid-Holocene (Cauquoin et al., 2019). In Renland and NGRIP simulated anomalies are slightly underestimated, in GRIP and GISP2 anomalies are slightly overestimated. But overall, the biases of the MPI-ESM-wiso mid-Holocene-PI model anomalies to the observed mid-Holocene-PI anomalies are for all ice cores very small.

3.2.2 $\delta^{18}O$ variability

The fact that, in contrast to the present-day simulations, only four observational data sets are available for the mid-Holocene, makes the assessment of the simulation results difficult. Moreover, the GRIP and GISP2 ice cores being located very close to each other (Figure 9), only three local isotope distributions clearly different from each other are available. Therefore, in Figure 9a, the spatial $\delta^{18}O$ variability of the COSMO_iso_50km simulation is illustrated for whole Greenland, which is, in accordance to the analysis of the present-day simulation, again calculated as the standard deviation of all COSMO_iso_50km grid boxes within the respective GCM grid boxes. In general, the $\delta^{18}O$ variability of COSMO_iso_50km in the mid-Holocene is high at the coastline, while it is lower in Central Greenland. The Renland ice core is consequently located in an area of a high isotopic variability, the GRIP and GISP2 ice cores in an area of low isotopic variability. But regions with increased isotopic variability occur also in the inland plateau of Greenland. The NGRIP ice core, for instance, is located in such an area of a moderate isotopic ratio variability. The four ice core drill sites are therefore located in three regions of Greenland with substantially different sub-grid isotopic ratio variabilities.

The spatial surface temperature variability in the COSMO_iso_50km mid-Holocene simulation is shown in Figure 9b. The mid-Holocene simulation shows a high spatial surface temperature variability near the coastline and almost no variability in Central Greenland. As a consequence, the spatial $\delta^{18}O$-temperature slope is low at the coastline and high in Central Greenland (Figure 9c). Moreover, the interannual $\delta^{18}O$-temperature slope is very small over Greenland in the mid-Holocene, although in some regions high temporal slopes are simulated (Figure 9d). But in principle, the influence of interannual surface temperature variations on the temporal $\delta^{18}O$ variability in the mid-Holocene is small.

In general, the results of the COSMO_iso_50km mid-Holocene simulation exhibit the same spatial characteristics as for the present-day simulation (Figure 7 and Figure 9). Comparable spatial patterns are simulated for the surface temperature variability (Figure 7b and Figure 9b) as well as the $\delta^{18}O$ variability (Figure 7a and Figure 9a) within a GCM grid box, although regions of increased $\delta^{18}O$ variability in Central Greenland are more widely present in the mid-Holocene run than in the present-day one. The contrast in the spatial $\delta^{18}O$-temperature slope between the coastal regions and the inland plateau is therefore in the mid-Holocene less clearly pronounced than under present-day conditions (Figure 7c and Figure 9c). Nevertheless, the spatial $\delta^{18}O$-temperature interrelations are in both periods comparable. This is also the case for the temporal variabilities of $\delta^{18}O$ and the surface temperature (Figure 7d and Figure 9d). This broad consistency in the

COSMO_iso_50km simulation results for the mid-Holocene and the present-day is remarkable, considering that both simulations are driven by two different forcing approaches (ECHAM5-wiso nudged to ERA-Interim reanalysis with prescribed monthly varying oceanic boundary conditions vs. the fully-coupled atmosphere-ocean Earth-System-Model MPI-ESM-wiso). This finding indicates that the spatial and interannual $\delta^{18}O$ variability of COSMO_iso_50km within a GCM grid box over Greenland is independent of the oceanic boundary conditions.

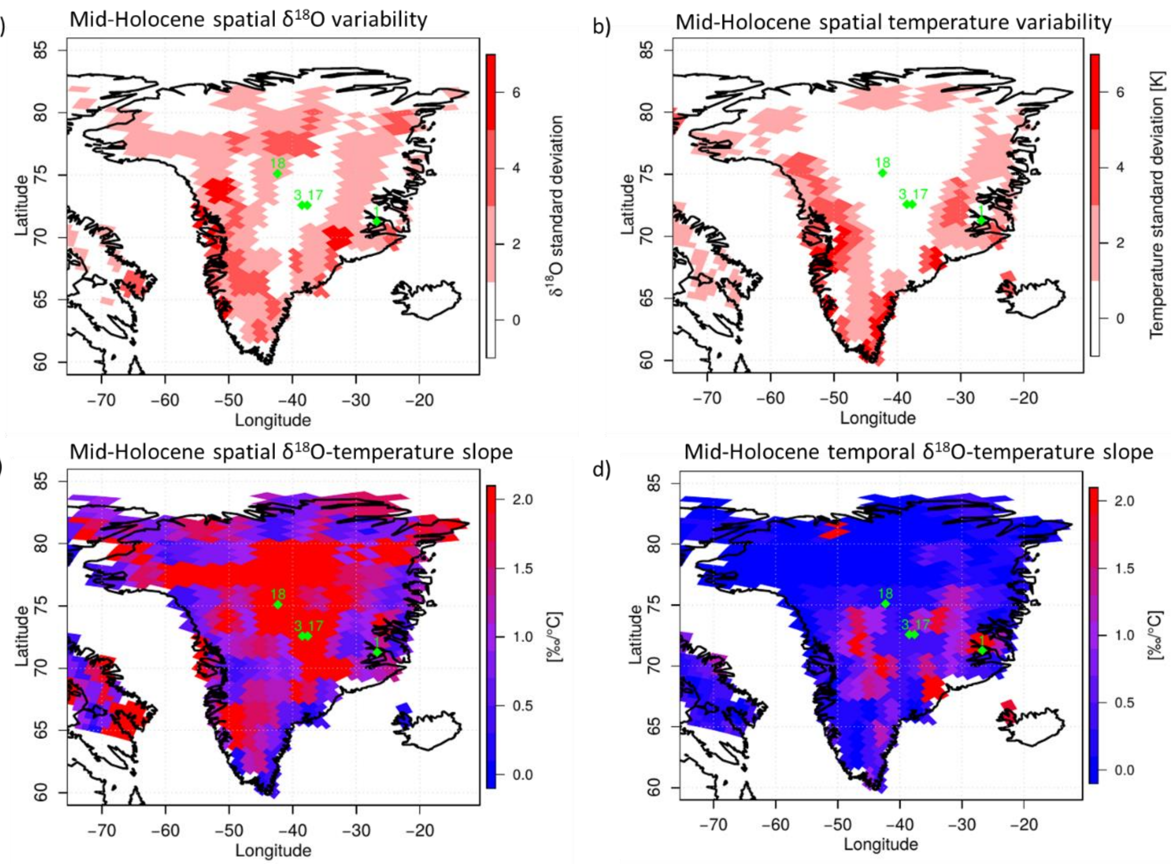

Figure 9: As Figure 7, but for the Mid-Holocene. The locations of the ice core samples are shown in blue.

4 Discussion and Conclusions

The results of several global paleo-climate simulations exhibit considerable deviations to the observed regional climate patterns during the Holocene (Braconnot et al., 2012). In the presented study, for the first time, regional climate simulations with an isotope-enabled RCM are performed for Greenland to potentially improve the agreement with climate observations in this region for the mid-Holocene. In a first step, the capability of the isotope-enabled RCM COSMO_iso to reproduce observed isotopic ratios for Greenland is demonstrated.

The COSMO_iso simulation results show that a spatial resolution of 50 km already leads to reasonable $\delta^{18}O$ values. Especially in regions where the global ECHAM5-wiso model, which has been used to derive necessary forcing fields for the COSMO_iso simulations, deviates strongly from the observed $\delta^{18}O$ values, the bias is considerably reduced by the regional climate simulation with COSMO_iso. In complex terrain like the coastal areas of Greenland, the results can be further improved with an additional downscaling to a spatial resolution of 7 km. In such simulations with high spatial resolution, small-scale processes are described in more detail (e.g. Torma et al., 2015; Coppola et al., 2018) and thus the local characteristics at ice core sites are better taken into account (Sturm et al., 2005; Werner et al., 2011). But for northern Greenland, regional climate simulations with COSMO_iso increase the bias with respect to observations. A comparison of simulated isotope ratios in precipitation with measured values at GNIP stations shows that such deviations between model results and observations are not caused by systematic seasonal biases in the RCM, as it was simulated by Sjolte et al., (2011) for Greenland. In central northern Greenland, rather a model bias is introduced, due to a southward shift of the area of low yearly mean $\delta^{18}O$ values. But all in all, the results of this study show that COSMO_iso is generally able to provide reasonable isotopic ratios for Greenland and the model can be applied for paleo-climate simulations.

For the mid-Holocene, MPI-ESM-wiso is in good agreement with observed ice core data in Greenland, as already described by Cauquoin et al. (2019). The model bias is, in this context, not further reduced by a downscaling with COSMO_iso. But an increase in the spatial model resolution leads also to an increase in the models' degrees of freedom. This in turn can lead to additional noise and thus, a deviating RCM behaviour with even an increase in the absolute model bias, as seen for the Renland station.

Another consequence of these increased degrees of freedom in the COSMO_iso simulation is that the spatial variability of the simulated $\delta^{18}O$ ratios is enhanced. This enhanced spatial variability represents the subgrid-scale uncertainty of the driving GCM, which can be derived in a physically consistent way by a regional downscaling. Now, by analysing this subgrid-scale variability, the spatial uncertainties in the comparison between GCM data and point measurements can be considered. In this way, it can be demonstrated that most of the observed $\delta^{18}O$ values lie within the local $\delta^{18}O$ uncertainties of the coarse GCM results. This applies for both, the present-day runs and the regional paleo-climate simulations for the mid-Holocene in Greenland. The deviation between the coarser resolved GCM results and the finer resolved observations is therefore potentially caused by the missing representation of important small-scale processes, which are induced by e.g. the surface conditions or orographic effects over Greenland. Shi et al., (2020), for instance, were able to demonstrate that GCM deficiencies to reproduce the observed water isotope variability in the southeastern Tibetan Plateau are associated with the missing representation of such small-scale processes in coarse GCM simulations.

As $\delta^{18}O$ ratios are used as an indicator for temperatures in past climates (Dansgaard et al., 1969; Masson-Delmotte et al., 2005; Jouzel, 2013), it is important to understand how the presented COSMO_iso simulations might be able to improve these isotope-based temperatures reconstructions. In general, the regional surface temperature variability and the regional $\delta^{18}O$

variability show similar patterns for Greenland. In both cases the variability is high at the coast and low on the inland plateau. Similar patterns as in the mid-Holocene can also be seen for the present-day simulations. These spatial variability patterns of $\delta^{18}O$ and the surface temperature are in line with the results of Sjolte et al. (2011) for RCM simulations under present-day conditions for Greenland. Based on these variability patterns, it can be derived that the regional surface temperature variability highly depends on the surface characteristics in Greenland. However, for the regional isotopic ratio variability, this dependence appears to be less pronounced. At the coastline, a clear relationship between surface temperatures and measured $\delta^{18}O$ ratios in ice cores can be deduced, while in Central Greenland this relation is weaker. These spatial differences might be explained by the fact that isotope changes are an integrated signal of the meso-scale variability of atmospheric processes (Dansgaard, 1964; Merlivat and Jouzel, 1979; Gat, 1996), which might partially be decoupled from surface temperature changes in homogeneous terrain.

Consistent structures over Greenland are also modelled for the interannual temporal $\delta^{18}O$-temperature slope in the mid-Holocene and the present-day simulation. But in comparison to the spatial $\delta^{18}O$-temperature slope, the interannual temporal interrelations between the surface temperature and $\delta^{18}O$ are rather small. This weaker interannual $\delta^{18}O$-temperature slope is again in line with the results of Sjolte et al. (2011).

The presented study demonstrates that the isotope-enabled MPI-ESM-wiso - COSMO_iso model chain with realistically implemented stable water isotope fractionation processes constitutes a useful supplement to reconstruct regional paleo-climate conditions during the mid-Holocene in Greenland. By means of such an isotope-enabled GCM-RCM model chain, locally measured isotope ratios in an ice core can be adequately linked to spatially coarse climate model results and conclusions on the underlying climatic processes leading to these ratios can be drawn in a physically consistent way. This approach might also be very helpful for other isotope-enabled GCMs and their deviations to observed isotope ratios in different paleo-time periods and regions. Particularly in regions, in which large differences occur between simulated and observed $\delta^{18}O$ ratios, due to small-scale orographic variations, like parts of Europe and North America (Cauquoin et al., 2019; Comas-Bru et al., 2019), an improved representation of small-scale processes can potentially reduce these biases, and consequently, the reconstruction of regional paleo-climate patterns can become more reliable. To test this hypothesis, in follow-up studies, more time slices will be simulated with the presented MPI-ESM-wiso – COSMO_iso model chain for different periods and different regions.

Code availability. The isotope-enabled version COSMO_iso is available upon request from Marcus Breil. The code of the isotopic version MPI-ESM-wiso is available upon request on the AWI’s GitLab repository (https://gitlab.awi.de/mwerner/mpi-esm-wiso, Cauquoin et al., 2019).

Author contributions. MB performed the COSMO_iso mid-Holocene simulations, EC the COSMO_iso present-day simulation. The ECHAM5-wiso simulations were performed by MW, the MPI-ESM-wiso simulations by AC. MB analysed the presented model results and wrote the manuscript with contributions from all co-authors.

Competing interests. The authors declare that they have no conflict of interest.

Acknowledgements. This work was supported by the German Federal Ministry of Education and Research (BMBF) as a Research for Sustainability initiative (FONA) through PalMod project (FKZ: 01LP1511B). All simulations were performed at the German Climate Computing Center (DKRZ).

References

Aemisegger, F., J. K. Spiegel, S. Pfahl, H. Sodemann, W. Eugster, and H. Wernli: Isotope meteorology of cold front passages: A case study combining observations and modeling, *Geophysical Research Letters*, 42(13), 5652–5660, doi:10.1002/2015GL063988, 2015.

Ambach, W., Dansgaard, W., Eisner, H., and Moller, J.: The altitude effect on the isotopic composition of precipitation and glacier ice in the Alps, Tellus, 20, 595–600, doi:10.1111/j.2153-3490.1968.tb00402.x, 1968.

Baldauf M, Seifert A, Förstner J, Majewski D, Raschendorfer M: Operational convective-scale numerical weather prediction with the COSMO model: description and sensitivities. *Mon Weather Rev*, 139:3887−3905, 2011.

Bonne, J. L., and Coauthors: Resolving the controls of water vapour isotopes in the Atlantic sector. *Nature communications*, *10*(1), 1632, 2019.

Braconnot, P., and Coauthors: Evaluation of climate models using palaeoclimatic data. *Nature Climate Change*, *2*(6), 417, 2012.

Cauquoin, A., Werner, M. and Lohmann, G.: Water isotopes – climate relationships for the mid-Holocene and pre-industrial period simulated with an isotope-enabled version of MPI-ESM, *Clim. Past*, 15, 1913-1937, doi:10.5194/cp-15-1913-2019, 2019.

Comas-Bru, L., Harrison, S. P., Werner, M., Rehfeld, K., Scroxton, N., Veiga-Pires, C., and SISAL working group members: Evaluating model outputs using integrated global speleothem records of climate change since the last glacial, *Clim. Past*, 15, 1557–1579, https://doi.org/10.5194/cp-15-1557-2019, 2019.

Coppola, E., and Coauthors: A first-of-its-kind multi-model convection permitting ensemble for investigating convective phenomena over Europe and the Mediterranean. *Climate Dynamics*, 1-32, 2018.

Craig, H., and Gordon, L. I.: Deuterium and oxygen 18 variations in the ocean and marine atmosphere, Stable isotopes in oceanographic studies and paleotemperatures, 23. Pisa, Italy: Conoglio Nazionale delle Richerche, Labortorio di Geologia Nucleare, 1965.

Christner, E., M. Kohler, and M. Schneider: The influence of snow sublimation and meltwater evaporation on dD of water vapor in the atmospheric boundary layer of central Europe, *Atmospheric Chemistry and Physics*, 17(2), 1207–1225, doi:10.5194/acp-17-1207-2017, 2017.

Christner, E., and Coauthors: The climatological impacts of continental surface evaporation, rainout, and subcloud processes on δD of water vapor and precipitation in Europe. *Journal of Geophysical Research: Atmospheres*, *123*(8), 4390-4409, 2018.

Dansgaard, W.: The abundance of O18 in atmospheric water and water vapour. *Tellus*, *5*(4), 461-469, 1953.

Dansgaard, W.: Stable isotopes in precipitation. *Tellus*, *16*(4), 436-468, 1964.

Dansgaard, W., Johnsen, S. J., Møller, J., and Langway, C. C.: One thousand centuries of climatic record from Camp Century on the Greenland ice sheet. *Science*, *166*(3903), 377-380, 1969.

Dee, D. P., and Coauthors: The ERA-Interim reanalysis: Configuration and performance of the data assimilation system. *Quarterly Journal of the royal meteorological society*, *137*(656), 553-597, 2011.

Dütsch, M.: Stable water isotope fractionation processes in weather systems and their influence on isotopic variability on different time scales. Diss no. 23939, Ph.D. thesis, ETH Zurich, 2017.

Felzer, B., and Thompson, S. L.: Evaluation of a regional climate model for paleoclimate applications in the Arctic. *Journal of Geophysical Research: Atmospheres*, *106*(D21), 27407-27424, 2001.

Fischer, H., and Coauthors: Little ice age clearly recorded in northern Greenland ice cores. *Geophysical Research Letters*, *25*(10), 1749-1752, 1998.

Fischer, H.: Stable oxygen isotopes on snow pit ngt01C93 from the North Greenland Traverse. doi:10.1594/PANGAEA.133399, 2003.

Fischer, N., and Jungclaus, J. H.: Evolution of the seasonal temperature cycle in a transient Holocene simulation: orbital forcing and sea-ice. *Climate of the Past*, *7*, 1139-1148, 2011.

Furukawa, R., Uemura, R., Fujita, K., Sjolte, J., Yoshimura, K., Matoba, S., & Iizuka, Y.: Seasonal-Scale Dating of a Shallow Ice Core From Greenland Using Oxygen Isotope Matching Between Data and Simulation. *Journal of Geophysical Research: Atmospheres*, *122*(20), 10-873, 2017.

Gat, J. R.: Oxygen and hydrogen isotopes in the hydrological cycle. *Annual Review of Earth and Planetary Sciences*,24(1), 225–262.https://doi.org/10.1146/annurev.earth.24.1.225, 1996.

Grootes, P. M., and Stuiver, M.: Oxygen 18/16 variability in Greenland snow and ice with 10− 3-to 105-year time resolution. *Journal of Geophysical Research: Oceans*, *102*(C12), 26455-26470, 1997.

Gurney, S. D., and Lawrence, D. S. L.: Seasonal trends in the stable isotopic composition of snow and meltwater runoff in a subarctic catchment at Okstindan, Norway. *Hydrology Research*, *35*(2), 119-137, 2004.

Harrison, S. P., and Coauthors: Climate model benchmarking with glacial and mid-Holocene climates. *Climate Dynamics*, *43*(3-4), 671-688, 2014.

IAEA/WMO (2016), http://www-naweb.iaea.org/napc/ih/IHS resources gnip.html.

Johnsen, S. J., Clausen, H. B., Cuffey, K. M., Hoffmann, G., Schwander, J., & Creyts, T.: Diffusion of stable isotopes in polar firn and ice: the isotope effect in firn diffusion. In *Physics of ice core records* (pp. 121-140). Hokkaido University Press, 2000.

Jost, A., Lunt, D., Kageyama, M., Abe-Ouchi, A., Peyron, O., Valdes, P. J., and Ramstein, G.: High-resolution simulations of the last glacial maximum climate over Europe: a solution to discrepancies with continental palaeoclimatic reconstructions?. *Climate Dynamics*, *24*(6), 577-590, 2005.

Jouzel, J., and Merlivat, L.: Deuterium and oxygen 18 in precipitation: Modeling of the isotopic effects during snow formation. *Journal of Geophysical Research: Atmospheres*, *89*(D7), 11749-11757, 1984.

Jouzel, J.: A brief history of ice core science over the last 50 yr, *Clim. Past*, 9, 2525–2547, 2013.

Jungclaus, J. H., Fischer, N., Haak, H., Lohmann, K., Marotzke,J., Matei, D., Mikolajewicz, U., Notz, D., and von Storch, J. S.: Characteristics of the ocean simulations in the Max Planck Institute Ocean Model (MPIOM) the ocean component of the MPI-Earth system model, J. Adv. Model. Earth Sy., 5, 422–446,https://doi.org/10.1002/jame.20023, 2013.

Kageyama, M., and Coauthors: The PMIP4 contribution to CMIP6–Part 1: Overview and over-arching analysis plan, *Geosci. Model Dev*., 11, 1033–1057, 2018.

Karremann, M.K., and Schädler, G.: Parametrisation of variables having an impact on the Greenland surface mass balance using regional climate model simulations, to be submitted to Atmosphere.

Marcott, S. A., Shakun, J. D., Clark, P. U., and Mix, A. C.: A reconstruction of regional and global temperature for the past 11,300 years. *Science*, *339*(6124), 1198-1201, 2013.

Masson-Delmotte, V., and Coauthors: GRIP deuterium excess reveals rapid and orbital-scale changes in Greenland moisture origin. *Science*, *309*(5731), 118-121, 2005.

Masson-Delmotte, V., and Coauthors: Recent changes in north-west Greenland climate documented by NEEM shallow ice core data and simulations, and implications for past-temperature reconstructions. The Cryosphere Discussions, Copernicus, 2015, pp.1481-1504. 10.5194/tc-9-1481-2015, 2015.

Merlivat, L., and Jouzel, J.: Global climatic interpretation of the deuterium-oxygen 18 relationship for precipitation. *Journal of Geophysical Research: Oceans*, *84*(C8), 5029-5033, 1979.

Moossen, H., Bendle, J., Seki, O., Quillmann, U., and Kawamura, K.: North Atlantic Holocene climate evolution recorded by high-resolution terrestrial and marine biomarker records. *Quaternary Science Reviews*, *129*, 111-127, 2015.

Pfahl, S., Wernli, H., and Yoshimura, K.: The isotopic composition of precipitation from a winter storm–a case study with the limited-area model COSMOiso. *Atmos. Chem. Phys*, *12*(3), 1629-1648, 2012.

Rockel, B., Will, A., and Hense, A.: The regional climate model COSMO-CLM (CCLM). *Meteorologische Zeitschrift*, *17*(4), 347-348, 2008.

Schrodin, R., and E. Heise: The multi-layer version of the DWD soil model TERRA-LM, Consortium for Small-Scale Modelling (COSMO) Tech. Rep., 2, 16, 2001.

Shi, X., and Coauthors: Variability of isotope composition of precipitation in the Southeastern Tibetan Plateau from the synoptic to seasonal time scale. *Journal of Geophysical Research: Atmospheres*, *125*(6), e2019JD031751, 2020.

Sjolte, J., Hoffmann, G., Johnsen, S. J., Vinther, B. M., Masson-Delmotte, V., and Sturm, C.: Modeling the water isotopes in Greenland precipitation 1959–2001 with the meso-scale model REMO-iso. *Journal of Geophysical Research: Atmospheres*, *116*(D18), 2011.

Smith, R. S., and Gregory, J.: The last glacial cycle: transient simulations with an AOGCM. *Climate dynamics*, *38*(7-8), 1545-1559, 2012.

Steen-Larsen, H. C., and Coauthors: What controls the isotopic composition of Greenland surface snow? *Climate of the Past*, 10(1), 377–392, 2014.

Steig, E. J., and Coauthors: High-resolution ice cores from US ITASE (West Antarctica): development and validation of chronologies and determination of precision and accuracy. *Annals of Glaciology*, *41*, 77-84, 2005.

Stevens, B., and Coauthors: Atmospheric component of the MPI-M earth system model: ECHAM6. *Journal of Advances in Modeling Earth Systems*, *5*(2), 146-172, 2013.

Sturm, K., Hoffmann, G., Langmann, B., and Stichler, W.: Simulation of δ18O in precipitation by the regional circulation model REMOiso. *Hydrological Processes: An International Journal*, *19*(17), 3425-3444, 2005.

Sturm, C., Hoffmann, G., and Langmann, B.: Simulation of the stable water isotopes in precipitation over South America: Comparing regional to global circulation models. *Journal of climate*, *20*(15), 3730-3750, 2007.

Timm, O., and Timmermann, A.: Simulation of the last 21 000 years using accelerated transient boundary conditions. *Journal of Climate*, *20*(17), 4377-4401, 2007.

Torma, C., Giorgi, F., and Coppola, E.: Added value of regional climate modeling over areas characterized by complex terrain—Precipitation over the Alps. *Journal of Geophysical Research: Atmospheres*, *120*(9), 3957-3972, 2015.

Vinther, B. M., and Coauthors: A synchronized dating of three Greenland ice cores throughout the Holocene. *Journal of Geophysical Research: Atmospheres*, *111*(D13), 2006.

Vinther, B. M., and Coauthors: Synchronizing ice cores from the Renland and Agassiz ice caps to the Greenland Ice Core Chronology. *Journal of Geophysical Research: Atmospheres*, *113*(D8), 2008.

von Storch, H., H. Langenberg, and F. Feser: A Spectral Nudging Technique for Dynamical Downscaling Purposes, *Monthly Weather Review*, 128(10), 3664–3673, doi:10.1175/1520-0493(2000)128¡3664:ASNTFD¿2.0.CO;2, 2000.

Weißbach, S., A. Wegner, T. Opel, H. Oerter, B. M. Vinther, and S. Kipfstuhl: Accumulation rate and stable oxygen isotope ratios of the ice cores from the North Greenland Traverse, doi:10.1594/PANGAEA.849161, 2016a.

Weißbach, S., Wegner, A., Opel, T., Oerter, H., Vinther, B. M., and Kipfstuhl, S.: Spatial and temporal oxygen isotope variability in northern Greenland–implications for a new climate record over the past millennium. *Climate of the Past*, *12*, 171-188, 2016b.

Werner, M., Langebroek, P. M., Carlsen, T., Herold, M., and Lohmann, G.: Stable water isotopes in the ECHAM5 general circulation model: Toward high-resolution isotope modeling on a global scale. *Journal of Geophysical Research: Atmospheres*, *116*(D15), 2011.

Yoshimori, M., and Suzuki, M.: The relevance of mid-Holocene Arctic warming to the future. *Climate of the Past*, *15*(4), 1375-1394, 2019.